

Surface characteristics and osteoblastic cell response of alkali- and heat-treated titanium-8tantalum-3niobium alloy

Bo-Ah Lee^{1,†}, Choong-Hee Kang^{2,†}, Mong-Sook Vang², Young-Suk Jung¹, Xing Hui Piao¹, Ok-Su Kim¹, Hyun-Ju Chung¹, Young-Joon Kim^{1,*}

¹Department of Periodontology, Dental Research Institute, Chonnam National University School of Dentistry, Gwangju, Korea

²Department of Prosthodontics, Chonnam National University School of Dentistry, Gwangju, Korea

Purpose: The aim of the present study was to evaluate the biological response of alkali- and heat-treated titanium-8tantalum-3niobium surfaces by cell proliferation and alkaline phosphatase (ALP) activity analysis.

Methods: Commercial pure titanium (group cp-Ti) and alkali- and heat-treated titanium-8tantalum-3niobium (group AHT) disks were prepared. The surface properties were evaluated using scanning electron microscopy, energy dispersed spectroscopy and X-ray photoelectron spectroscopy (XPS). The surface roughness was evaluated by atomic force microscopy and a profilometer. The contact angle and surface energy were also analyzed. The biological response of fetal rat calvarial cells on group AHT was assessed by cell proliferation and ALP activity.

Results: Group AHT showed a flake-like morphology microprofile and dense structure. XPS analysis of group AHT showed an increased amount of oxygen in the basic hydroxyl residue of titanium hydroxide groups compared with group cp-Ti. The surface roughness (Ra) measured by a profilometer showed no significant difference ($P > 0.05$). Group AHT showed a lower contact angle and higher surface energy than group cp-Ti. Cell proliferation on group AHT surfaces was significantly higher than on group cp-Ti surfaces ($P < 0.05$). In comparison to group cp-Ti, group AHT enhanced ALP activity ($P < 0.05$).

Conclusions: These results suggest that group AHT stimulates osteoblast differentiation.

Keywords: Alkaline phosphatase, Cell adhesion, Cell proliferation, Surface properties, Titanium alloy.

INTRODUCTION

Titanium and titanium alloys are among the most popular materials for dental and orthopedic implants due to their biocompatibility, excellent resistance to corrosion, and good mechanical properties [1]. One of the key factors for success with load-bearing dental implants is prompt, long-lasting implant stability. In most cases this stability relies on a high degree of implant osseointegration [2]. There have been ongoing efforts

to improve the osseointegration capability of titanium implants by enhancing the osteoconduction on their surfaces using surface morphology and chemistry [3-5].

A variety of techniques have been developed to produce microrough titanium surfaces that promote bone ingrowth and fixation between the implants and bone. Surface blasting, acid-etching and combinations of the two are widely used methods for modification of the surface topography. These modified surfaces demonstrate enhanced bone apposition

Received: Nov. 9, 2012; **Accepted:** Nov. 13, 2012

***Correspondence:** Young-Joon Kim

Department of Periodontology, Chonnam National University School of Dentistry, 77 Yongbong-ro, Buk-gu, Gwangju 500-757, Korea

E-mail: youngjun@chonnam.ac.kr, Tel: +82-62-530-5648, Fax: +82-62-530-5649

[†]These authors contributed equally to this study.

on histomorphometric studies, and higher removal torque values on biomechanical testing [3,4]. In addition to the surface topography, surface chemistry is another key variable for peri-implant bone apposition. Kokubo et al. [4] introduced an alkaline- and heat-treated titanium surface that provides strong bone-bonding with high bone affinity. After the alkaline and heat treatments, titanium-based metals form bone-like apatite in simulated body fluid (SBF), which has ion concentrations nearly equal to human body fluids [5]. This phenomenon also occurs on the surfaces of bioactive glass and glass ceramics.

Osteoblasts are cells that respond to their substrate and rely heavily on signals to maintain the osteoblast phenotype. If insufficient signals are provided by the substrate, a fibroblast phenotype develops [6]. Other inflammatory mediators also regulate cell activity, as do other molecules such as osteoprotegerin and the receptor activator of nuclear factor kappa B ligand [7].

Prior studies have found that titanium prepared by alkali treatment could form bone-like apatite when soaked in SBF *in vitro*, and had a strong bone-bonding ability and high bone affinity *in vivo* [4,8-11]. These features of alkali- and heat-treated titanium alloys suggest the possibility of an alkali- and heat-treated titanium alloy as a candidate for use in the preparation of medical devices.

The way in which osteoblasts or osteogenic cells react with alkali- and heat-treated surfaces has not yet been clarified. Osteoblasts may attach to the apatite formed on the alkali- and heat-treated surfaces, and this may enhance growth and differentiation. As osteoblasts are pivotal to bone remodeling, a biological response can help to delineate the action of alkali- and heat-treated titanium alloys *in vitro*. Thus, the purpose of this study was to evaluate the surface characteristics and to describe the cellular events that follow cell adhesion to alkali- and heat-treated surfaces by cell proliferation and alkaline phosphatase (ALP) activity analysis.

MATERIALS AND METHODS

Sample preparation

In this study, commercially pure titanium (grade II, group cp-Ti) and alkali- and heat-treated titanium-8tantalum-3niobium (group AHT) samples were prepared as disks (12 mm diameter, 1 mm thickness). All disks were kindly provided by the Department of Materials Science and Engineering, Chonnam National University. The Cp-Ti disks were wet ground with 240, 400, and 600 grit silicon carbide paper. These surfaces were ultrasonically degreased in acetone and ethanol for 10 minutes each, and rinsed with de-ionized water between applications of each solvent. The alkali treatment was

performed by soaking the samples in a solution of 5 M NaOH at a temperature of 60°C for 24 hours. The samples were then cleaned ultrasonically for 10 minutes using distilled water and dried at 40°C for 24 hours. They were heated to 600°C with a heating rate of 5°C/min, kept at a given temperature for 1 hour, and then allowed to cool to room temperature in the furnace.

Surface characterization

The surface morphology and composition were analyzed by scanning electron microscopy (SEM; S-4700, Hitachi, Tokyo, Japan) and energy dispersed spectroscopy (EDS; Emax, Horiba, Kyoto, Japan). The surface composition was examined by X-ray photoelectron spectroscopy (XPS; Multilab 2000, Thermo Electron, Waltham, MA, USA). The surface roughness was evaluated by atomic force microscopy (AFM; NanoScope IIIa, Digital Instruments, Santa Barbara, CA, USA) and a profilometer (DIAVITE DH-7, Asmeto Ltd., Richterswil, Switzerland).

The contact angle of each sample was measured using an imaging analysis microscope (Camscope, Sometech Inc., Seoul, Korea). The contact angles were determined using drops of distilled water at room temperature. The image of the water droplet was captured at 30 seconds after delivery. The contact angle was analyzed with image analysis software (Surftens QA 3.0, OEG GmbH, Frankfurt, Germany).

The surface energy was calculated by the Good & Van Oss model using the following equation:

$$\gamma_{SL} = \gamma_S + \gamma_L - 2 \left[(\gamma_S^{LW} \gamma_L^{LW})^{1/2} + (\gamma_S^+ \gamma_L^-)^{1/2} + (\gamma_S^- \gamma_L^+)^{1/2} \right]$$

(γ_{SL} : solid-liquid interfacial tension, γ_S : solid-vapour interfacial tension, γ_L : liquid-vapour interfacial tension, γ_S^{LW} : Lifshitz-van der Waals component, γ_L^{LW} : Lifshitz-van der Waals component)

The surface energy analysis used the three-liquid method: distilled water, formaldehyde (polar solvent), and diiodomethane (nonpolar solvent). Surface free energy and its components of each solvent employed are presented in Table 1. The contact angle for each solvent was measured.

Table 1. Surface free energy and its components of liquids employed (mJ/m²).

	γ_L	γ_L^{LW}	γ_L^+	γ_L^-
Water	72.8	21.8	25.5	25.5
Diiodomethane	50.8	50.8	0	0
Ethylene glycol	48.0	29.0	1.92	47.0
Formamide	58.0	39.0	2.28	39.6

γ_L : liquid-vapour interfacial tension, γ_L^{LW} : Lifshitz-van der Waals component, γ_L^+ : liquid-vapour interfacial tension of electron donor, γ_L^- : liquid-vapour interfacial tension of electron acceptor.

Cell culture of fetal rat calvarial cells

Osteoblast-enriched cell preparations were obtained from 21-day fetal calvaria of Sprague-Dawley rats by sequential collagenase digestion (Type II, Gibco BRL, Grand Island, NY, USA) as described previously [12]. The cells resulting from the third to fifth 15-minute digestions were pooled and cultured in BGJb media (Gibco BRL) supplemented with 10% heat-inactivated fetal bovine serum (FBS, Gibco BRL), 100 mg/mL penicillin (Gibco BRL), and 100 mg/mL streptomycin (Gibco BRL) at 37°C in a humidified atmosphere with 5% CO₂-95% air.

Evaluation of cell adhesion

The cp-Ti and AHT were placed, under aseptic conditions, in the bottom of 12-well culture dishes, and then rinsed three times in 70% ethanol, exposed to ultraviolet light for 1 hour, and air dried in the cell culture hood.

The fetal rat calvarial cells were seeded at a density of 1×10^4 cells/mL in the BGJb media. After a 3-day incubation period, the dishes were washed three times with phosphate buffered saline (PBS, Gibco BRL), and fixed with 2.5% glutaraldehyde (Sigma-Aldrich Co., St. Louis, MO, USA) in 100 mM cacodylate buffer (Sigma-Aldrich Co.). The samples were dehydrated in increasing concentrations of ethanol (30%, 60%, 95%, and 100%), immersed in hexamethyldisilazane (Sigma-Aldrich Co.) for 15 minutes, air-dried, and immediately mounted on aluminum stubs and coated with carbon. SEM was then performed.

Evaluation of cell proliferation

Cell proliferation was assessed using a 3-(4,5-Dimethylthiazol-2-yl)-2,5-diphenyltetrazolium bromide (MTT) assay using the fetal rat calvarial cells. Cells were cultured on each disc in 12-well plate at a density of 1×10^4 cells/mL in the BGJb medium supplemented with 10% FBS. Following incubation, cell proliferation was assessed at 1, 3, and 5 days using a MTT assay (CellTiter 96, Aqueous One Solution, Promega, Madison, WI, USA). In these experiments, the amount of reduced formazan product is directly proportional to the number of viable cells. Formazan accumulation was quantitated by absorbance at 490 nm using an enzyme-linked immunoabsorbent assay plate reader (VERSAmass, Dynamic Devices, Wilmington, DE, USA). The experiment was carried out in triplicate.

ALP activity

ALP activity was measured spectrophotometrically using the fetal rat calvarial cells. The cells were seeded onto 12 well dishes at a density of 1×10^4 cell/mL in the BGJb medium containing 10% FBS, ascorbate 40 g/mL and 20 g/mL β -glycerol phosphate. After incubation for 7 days, the cells were washed with PBS, lysed in Triton 0.1% (Triton X-100, Promega) in PBS,

then frozen at -20°C and thawed. Then 100 g of the cell lysates was mixed with 200 g of 10 mM p-nitrophenyl phosphate and 100 g of 1.5 M 2-amino-2-methyl-1-propanol buffer (Sigma-Aldrich Co.). The samples were incubated for 1 hour at 37°C. The ALP activity was measured from the absorbance reading at 405 nm with a spectrophotometer (SmartSpec, Bio-Rad Laboratories Inc., Hercules, CA, USA) and corrected for the cell number determined in parallel. All experiments were carried out in triplicate.

Statistical analysis

An analysis of variance for repeated measurements were performed to examine the data for surface roughness, surface energy, contact angle measurement, cell proliferation, and ALP activity with SPSS ver. 12.0 (SPSS Inc., Chicago, IL, USA).

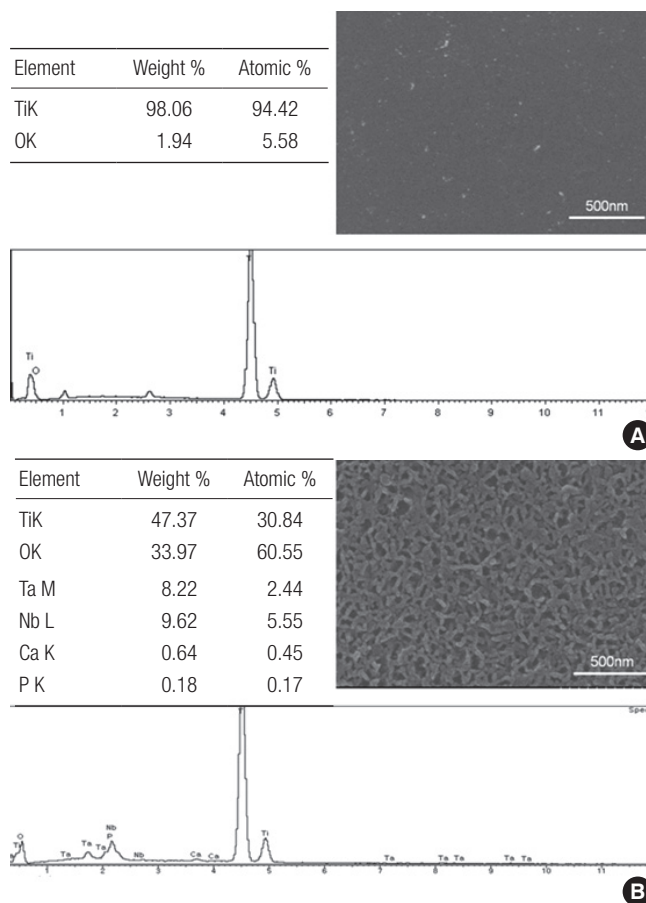


Figure 1. Scanning electron microscopy (SEM) and energy dispersed spectroscopy (EDS) analysis. (A) Commercially pure titanium (group cp-Ti) showed a uniform texture with porosity. EDS spectrum showed titanium and oxygen peak. (B) Alkali- and heat-treated titanium-8tantalum-3niobium (group AHT) showed a flake-like morphology microprofile and dense structure. The proportion of oxygen in the alkali- and heat-treated titanium was higher than that in the commercially pure titanium. Calcium and phosphor peaks were detected in EDS spectrum of group AHT but not in that of group cp-Ti.

The results were considered significant where $P < 0.05$.

RESULTS

Surface characterization

Fig. 1 shows the SEM images and EDS spectra of samples.

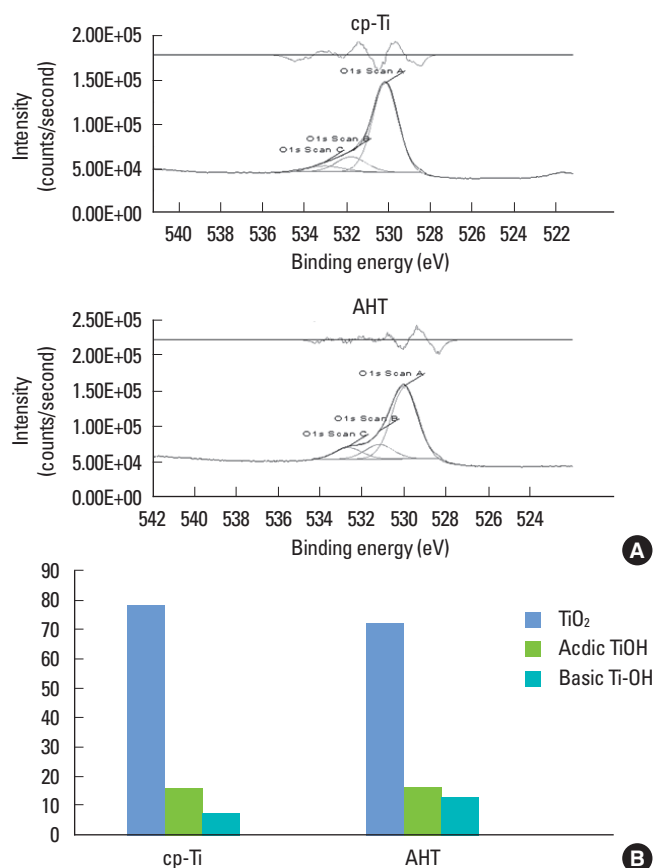


Figure 2. X-ray photoelectron spectroscopy analysis. (A) O1s spectra and (B) percentage of three oxygen species for commercially pure titanium (group cp-Ti) and alkali- and heat-treated titanium-8tantalum-3niobium (group AHT). Group AHT showed increased amount of hydroxyl groups on the surface layers. TiO₂: titanium dioxide, TiOH: acidic titanium hydroxyl group, Ti-OH: basic titanium hydroxyl group.

Group cp-Ti showed a uniform texture with porosity. The EDS spectrum showed titanium and oxygen peaks. Group AHT showed a flake-like morphology microprofile and dense structure. The proportion of oxygen in group AHT was higher than that in group cp-Ti. Calcium and phosphor peaks were detected in the EDS spectrum of group AHT, but not in that of group cp-Ti.

Fig. 2A shows the O1s XPS spectra for the surface of groups cp-Ti and AHT. The XPS spectra of O1s were classified into three Gaussian component peaks [13]. Titanium dioxide surfaces have two hydroxide groups: an acidic hydroxide group (531.1 eV, TiOH) and a basic hydroxide group (532.4 eV, Ti-OH). The TiOH group is acidic, whereas the Ti-OH group is basic and reacts readily with other anions. Fig. 2B shows the relative ratios of peak areas for oxygen in surface oxide lattices (denoted by TiO₂), oxygen in the hydroxyl residue of acidic titanium hydroxyl groups (bridging OH group, denoted by acidic TiOH) and oxygen in the hydroxyl residue of basic titanium hydroxyl groups (terminal OH group, denoted by basic Ti-OH). The alkali- and heat-treatment increased the amount of O in basic Ti-OH groups, meaning increased active OH groups on the surfaces.

Three-dimensional AFM images (5 × 5 μm) showed nanoscale roughness on alkali- and heat-treated surfaces (Fig. 3). The surface topography of group AHT had spike shape than group cp-Ti. The mean surface roughness (Ra) measured by AFM was greater on group AHT than on group cp-Ti (19.1 nm and 0.6 nm, respectively).

Despite this difference in microroughness, the surface roughness (Ra) measured by the profilometer showed no significant

Table 2. Contact angle and surface energy.

	cp-Ti	AHT
Contact angle	59.00 ± 5.27	32.02 ± 3.98
Surface energy (dyne/cm)	46.92 ± 4.04	64.68 ± 2.73

Values are presented as mean ± standard deviation.

cp-Ti: commercially pure titanium, AHT: alkali- and heat-treated titanium-8tantalum-3niobium.

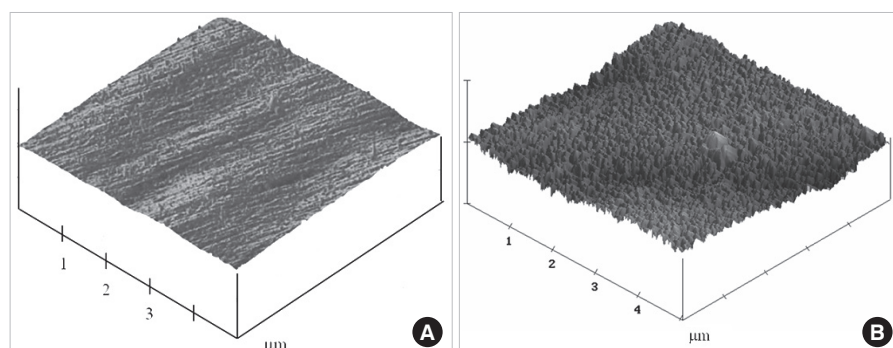


Figure 3. Atomic force microscopy (AFM) analysis of (A) commercially pure titanium (group cp-Ti) and (B) alkali- and heat-treated titanium-8tantalum-3niobium (group AHT). Three-dimensional AFM images (5 × 5 μm) showed nanoscale roughness on the group AHT surfaces. The surface topography of group AHT had more spike shape than the group cp-Ti.

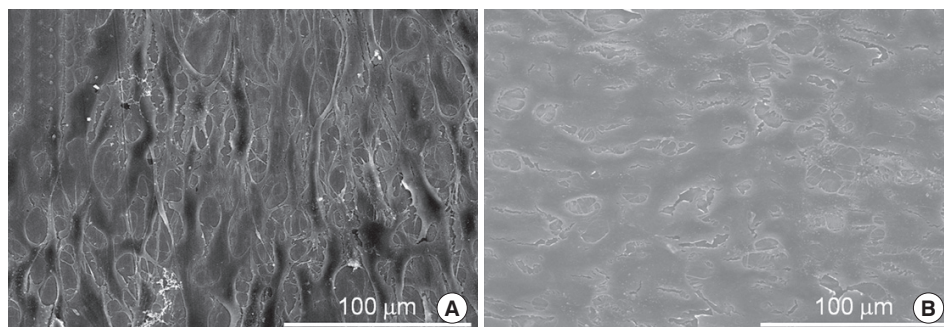


Figure 4. Cell adhesion examined by scanning electron microscopy (SEM). (A) The cells were spread extensively and totally flattened on the commercially pure titanium (group cp-Ti) surfaces. (B) The cells were spread extensively and totally flattened on the alkali- and heat-treated titanium-8tantalum-3niobium (group AHT). They were polygonal shapes with filopodial extensions, indicative of cell spreading. They did not have a regular orientation, and appeared scattered in all directions. The cells spread polygonally and cell projections connecting the cells were visible. No significant morphological difference was observed.

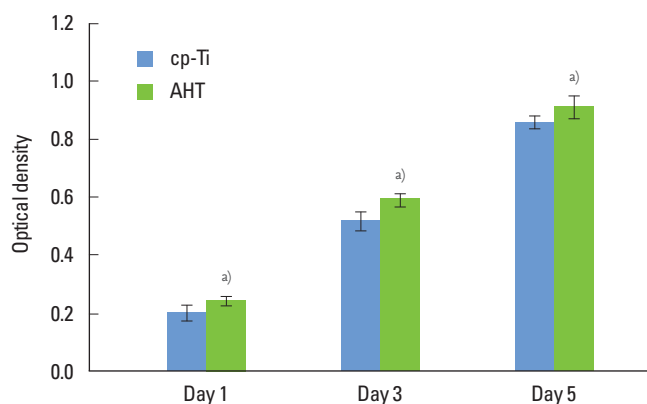


Figure 5. Cell proliferation measured by the 3-(4,5-Dimethylthiazol-2-yl)-2,5-diphenyltetrazolium bromide assay. On day 1, 3 and 5, the alkali- and heat-treated titanium-8tantalum-3niobium (group AHT) showed significantly greater cell proliferation compared with the commercial pure titanium (group cp-Ti). ^{a)}A statistically significant difference as compared with cp-Ti ($P < 0.05$).

difference (group cp-Ti, $0.31 \pm 0.07 \mu\text{m}$; group AHT, $0.34 \pm 0.06 \mu\text{m}$; $P > 0.05$).

Table 2 presents the contact angle and surface energy group AHT showed a lower contact angle and higher surface energy than group cp-Ti.

Cell responses

For each specimen, the cells were examined by SEM (Fig. 4). The cells were spread extensively and totally flattened on group AHT surfaces. They were polygonal shapes with filopodial extensions, indicative of cell spreading. They did not have a regular orientation, and appeared scattered in all directions. On group cp-Ti and group AHT surfaces, the cells spread polygonally and cell projections connecting the cells were visible. No significant morphological difference was observed between cells on the cp-Ti, and alkali- and heat-treated sur-

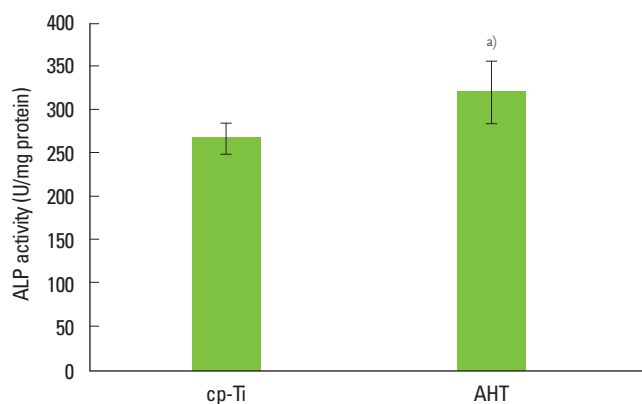


Figure 6. Alkaline phosphatase (ALP) activity on the alkali- and heat-treated titanium-8tantalum-3niobium (group AHT) was the higher than on the commercially pure titanium (group cp-Ti). ^{a)}A statistically significant difference as compared with cp-Ti ($P < 0.05$).

faces. Thus, we can conclude that group AHT did not disturb the cell attachment.

Cell proliferation was measured by the MTT assay (Fig. 5). On days 1, 3, and 5, group AHT showed a proliferation rate of 121%, 114%, and 106%, respectively, compared to group cp-Ti at the same respective points in time. The differences were statistically significant ($P < 0.05$).

The cells on group AHT showed 20% higher ALP activity than on the group cp-Ti (Fig. 6). The differences were statistically significant ($P < 0.01$).

DISCUSSION

Since alkali and heat treatment of titanium surfaces was introduced, it has been reported that an apatite layer is formed on the alkali- and heat-treated surface and this apatite layer is osteoconductive [10,11]. However, the cellular response of osteoblasts on the surface of those implants has not been re-

ported. In this study, the cellular response of group AHT was assessed by SEM, cell proliferation assay, and ALP activity analysis.

In this study, primary osteoblasts were obtained from fetal rat calvaria. This is an excellent source of osteoblasts because cells from young animals proliferate rapidly. Cells from the third, fourth, and fifth digests were collected because these later digests provide a more pure culture, containing mostly cells that express an osteoblast-like phenotype [14].

Surface roughness can greatly affect the proliferation and protein synthesis of osteoblast cells that are cultured on a metal substrate during bone healing [15,16]. Many studies have demonstrated that roughness significantly influences cell responses. In this study, the surface roughness measured with a profilometer showed no significant difference between group cp-Ti and AHT, although AFM and SEM analysis showed irregular surface morphology of group AHT. Nanoscale roughness shown in AFM images involves surface chemistry. Therefore, the enhanced cell response on alkali- and heat-treated surfaces might not be attributed to the surface roughness. Instead, it seemed that the difference in the microprofile and chemical properties contributed to an enhanced cell response.

The finding that the surface roughness was not affected by the alkali- and heat-treatment is important. It has been reported that an implant with a rough surface might show more pronounced progression of peri-implantitis than that of a smooth surface [17], although rough surfaces allow enhanced osseointegration [18]. In this regard, an alkali- and heat-treated implant might be more favorable for periimplant tissue health than an implant with a rough surface.

Alkali- and heat-treatment reduced the contact angle and increased the surface energy via alteration of surface chemical composition. The lower contact angle and higher surface energy create a hydroxylated and hydrophilic surface, and promote the adhesion of relevant proteins [19]. These properties can result in increased cell attachment and proliferation. The hydrophilicity is associated with abundant hydroxyl groups. In this study, XPS results showed that alkaline treatment increased the number of OH groups.

In addition, a thin reactive layer of Ca-P (Ca-P layer) formed on alkali- and heat-treated surfaces. This result is consistent with the findings of other reports [4,10,11,20,21]. A Ca-P layer can form apatite in SBF and enhance the differentiation of osteoblasts. Several researchers have suggested that the formation of apatite should be associated with the formation of titanium oxide layer following alkali treatment and its densification after heat treatment [20,22,23]. The apatite formed on alkali- and heat-treated surfaces would bind chemically to the apatite in the bone. In the present study, EDS analysis revealed

the presence of calcium and phosphorus on an alkali- and heat-treated surface. In addition, SEM analysis showed a dense structure of an alkali- and heat-treated surface. The Ti-OH groups formed on the surface are negatively charged and combine selectively with the positively charged Ca^{2+} ions in the fluid [24]. As a result, a positively charged surface combines with negatively charged phosphate ions to form an amorphous calcium phosphate. This calcium phosphate spontaneously transforms into the crystalline apatite.

The cell morphology was examined by SEM. The SEM evaluations showed that the cells spread extensively and flattened on the group cp-Ti and AHT surfaces. The absence of significant morphological modification supports the cytocompatibility of these metals. The lower contact angle, meaning higher wettability, would promote cell spreading and attachment on the surface group AHT. Surface hydrophilicity is a factor that determines biocompatibility of biomaterials and is largely dependent on surface energy [25].

The cell proliferation on the group AHT surface was significantly greater than on the group cp-Ti surface on days 1, 3, and 5. The lower contact angle and higher surface energy created a hydroxylated and hydrophilic surface, promoted the adhesion of relevant proteins, and increased cell attachment and proliferation [19].

In addition to increased cell proliferation, group AHT showed a higher level of ALP activity. The hydroxylated surface can form a calcium phosphate layer in SBF, which enhances the differentiation of osteoblasts [20]. The enhancement of ALP activity would contribute to the facilitation of osteoblastic differentiation.

Osteoblast cells undergo a temporal sequence with a change of phase during the development of their completely differentiated phenotype: proliferation, differentiation, and mineralization [26]. Cells initially increase their number and produce an extracellular matrix. The phase of differentiation follows, characterized by the production of high levels of ALP, and modifications of the matrix that lead to the deposition of hydroxyapatite crystals. Cells grown on group AHT showed ALP levels significantly higher than on group cp-Ti ($P < 0.05$). ALP is an enzyme belonging to the group of membrane-bound glycoproteins. Although its physiological function remains unclear, ALP may play a key role in the formation and calcification of hard tissues [27]. Its expression and enzyme activity are frequently used as markers for osteoblast cells. This finding is consistent with the results reported by Chosa et al. [28], and could be explained by the alkali- and heat-treated surface increasing osteoblastogenesis and bone formation.

The results of this study have shown that group AHT had a better cell response than cp-Ti for bone remodeling. Therefore, group AHT might be a candidate for use in the prepara-

tion of medical and dental devices. However, additional animal and human studies are needed before using this alloy in the clinical setting.

Osseointegration of dental implants depends on the cell responses around the implant. The changes in osteoblast proliferation, differentiation, and maturation are important events in bone remodeling. Group AHT formed an apatite surface layer that facilitated osteogenic differentiation. Since osteoblasts are central to bone remodeling, a biological response should be demonstrated to clarify the activity of group AHT *in vitro*.

In summary, these results show that alkali- and heat-treatment enhances cell proliferation and ALP activity, suggesting that group AHT may stimulate osteoblast differentiation and consequently facilitate bone remodeling.

CONFLICT OF INTEREST

No potential conflict of interest relevant to this article was reported.

ACKNOWLEDGEMENTS

This study was financially supported by research fund of Chonnam National University in 2010.

REFERENCES

1. Park JB, Lakes RS. Biomaterials: an introduction. 2nd ed. New York: Kluwer Academic Publishers; 1992.
2. Cochran DL, Schenk RK, Lussi A, Higginbottom FL, Buser D. Bone response to unloaded and loaded titanium implants with a sandblasted and acid-etched surface: a histometric study in the canine mandible. *J Biomed Mater Res* 1998;40:1-11.
3. Li D, Ferguson SJ, Beutler T, Cochran DL, Sittig C, Hirt HP, et al. Biomechanical comparison of the sandblasted and acid-etched and the machined and acid-etched titanium surface for dental implants. *J Biomed Mater Res* 2002;60:325-32.
4. Kokubo T, Miyaji F, Kim HM, Nakamura T. Spontaneous formation of bonelike apatite layer on chemically treated titanium metals. *J Am Ceram Soc* 1996;79:1127-9.
5. Shi S, Kirk M, Kahn AJ. The role of type I collagen in the regulation of the osteoblast phenotype. *J Bone Miner Res* 1996;11:1139-45.
6. Sisk MA, Lohmann CH, Cochran DL, Sylvia VL, Simpson JP, Dean DD, et al. Inhibition of cyclooxygenase by indomethacin modulates osteoblast response to titanium surface roughness in a time-dependent manner. *Clin Oral Implants Res* 2001;12:52-61.
7. de Groot K, Wolke JG, Jansen JA. Calcium phosphate coatings for medical implants. *Proc Inst Mech Eng H* 1998;212:137-47.
8. Nishiguchi S, Nakamura T, Kobayashi M, Kim HM, Miyaji F, Kokubo T. The effect of heat treatment on bone-bonding ability of alkali-treated titanium. *Biomaterials* 1999;20:491-500.
9. Nishiguchi S, Kato H, Neo M, Oka M, Kim HM, Kokubo T, et al. Alkali- and heat-treated porous titanium for orthopedic implants. *J Biomed Mater Res* 2001;54:198-208.
10. Nishiguchi S, Fujibayashi S, Kim HM, Kokubo T, Nakamura T. Biology of alkali- and heat-treated titanium implants. *J Biomed Mater Res A* 2003;67:26-35.
11. Green J, Schotland S, Stauber DJ, Kleeman CR, Clemens TL. Cell-matrix interaction in bone: type I collagen modulates signal transduction in osteoblast-like cells. *Am J Physiol* 1995;268(5 Pt 1):C1090-103.
12. McCarthy TL, Centrella M, Canalis E. Further biochemical and molecular characterization of primary rat parietal bone cell cultures. *J Bone Miner Res* 1988;3:401-8.
13. Healy KE, Ducheyne P. Hydration and preferential molecular adsorption on titanium *in vitro*. *Biomaterials* 1992;13:553-61.
14. Luben RA, Wong GL, Cohn DV. Biochemical characterization with parathormone and calcitonin of isolated bone cells: provisional identification of osteoclasts and osteoblasts. *Endocrinology* 1976;99:526-34.
15. Lincks J, Boyan BD, Blanchard CR, Lohmann CH, Liu Y, Cochran DL, et al. Response of MG63 osteoblast-like cells to titanium and titanium alloy is dependent on surface roughness and composition. *Biomaterials* 1998;19:2219-32.
16. Kawahara H, Soeda Y, Niwa K, Takahashi M, Kawahara D, Araki N. *In vitro* study on bone formation and surface topography from the standpoint of biomechanics. *J Mater Sci Mater Med* 2004;15:1297-307.
17. Berglundh T, Gotfredsen K, Zitzmann NU, Lang NP, Lindhe J. Spontaneous progression of ligature induced peri-implantitis at implants with different surface roughness: an experimental study in dogs. *Clin Oral Implants Res* 2007;18:655-61.
18. Abrahamsson I, Berglundh T, Linder E, Lang NP, Lindhe J. Early bone formation adjacent to rough and turned endosseous implant surfaces. An experimental study in the dog. *Clin Oral Implants Res* 2004;15:381-92.
19. Pesskova V, Kubies D, Hulejova H, Himmlova L. The influence of implant surface properties on cell adhesion and proliferation. *J Mater Sci Mater Med* 2007;18:465-73.
20. Sultana R, Kon M, Hirakata LM, Fujihara E, Asaoka K, Ichikawa T. Surface modification of titanium with hydrother-

- mal treatment at high pressure. *Dent Mater J* 2006;25:470-9.
21. Jonasova L, Muller FA, Helebrant A, Strnad J, Greil P. Biomimetic apatite formation on chemically treated titanium. *Biomaterials* 2004;25:1187-94.
 22. Kim HM, Miyaji F, Kokubo T, Nishiguchi S, Nakamura T. Graded surface structure of bioactive titanium prepared by chemical treatment. *J Biomed Mater Res* 1999;45:100-7.
 23. Kim HM, Miyaji F, Kokubo T, Nakamura T. Effect of heat treatment on apatite-forming ability of Ti metal induced by alkali treatment. *J Mater Sci Mater Med* 1997;8:341-7.
 24. Tamilselvi S, Raghavendran HB, Srinivasan P, Rajendran N. In vitro and in vivo studies of alkali- and heat-treated Ti-6Al-7Nb and Ti-5Al-2Nb-1Ta alloys for orthopedic implants. *J Biomed Mater Res A* 2009;90:380-6.
 25. Zhao G, Schwartz Z, Wieland M, Rupp F, Geis-Gerstorfer J, Cochran DL, et al. High surface energy enhances cell response to titanium substrate microstructure. *J Biomed Mater Res A* 2005;74:49-58.
 26. Lian JB, Stein GS. The developmental stages of osteoblast growth and differentiation exhibit selective responses of genes to growth factors (TGF beta 1) and hormones (vitamin D and glucocorticoids). *J Oral Implantol* 1993;19:95-105.
 27. Genge BR, Sauer GR, Wu LN, McLean FM, Wuthier RE. Correlation between loss of alkaline phosphatase activity and accumulation of calcium during matrix vesicle-mediated mineralization. *J Biol Chem* 1988;263:18513-9.
 28. Chosa N, Taira M, Saitoh S, Sato N, Araki Y. Characterization of apatite formed on alkaline-heat-treated Ti. *J Dent Res* 2004;83:465-9.